Electronic Supplementary Material (ESI) for Nanoscale Advances.

Quantifying the removal of stabilizing thiolates from gold nanoparticles on different carbon supports and the effect on their electrochemical properties

Emil Dieterich, Simon-Johannes Kinkelin, Matthias Steimecke and Michael Bron*

Institut für Chemie, Technische Chemie I

Martin-Luther-Universität Halle-Wittenberg

Von-Danckelmann-Platz 4, 06120 Halle, Germany

E-mail: *michael.bron@chemie.uni-halle.de

Supporting information

1. Additional experimental details

1.1. Glassware cleaning with aqua regia

All glassware was cleaned with aqua regia before use. Flasks where filled with aqua regia, while vessels etc. where submerged in aqua regia and stirred for at least 12 h under reflux. Afterwards the temperature was increased in steps of 5 °C every 20 min up to 50 °C which was hold for 1 h. Finally the flasks where filled with DI water, vessels etc. where submerged in DI water and the temperature was increased until boiling and kept there for at least 30 min with reflux cooling.

1.2. Treatment of supporting materials as reference materials for TG-MS

The Vulcan carbon and the pre-treated CNT and BP2000 were treated with 15 % H_2/Ar at 400 °C for 1 h or 20 % O_2/Ar at 300 °C for 1 h or with both treatments combined, in the same way as the Au/C catalysts. Afterwards they were investigated by TG-MS in order to determine the amount of liberated SO_2, which was then used for correcting the results of Au/C.

1.3. TG-MS SO_2 area correction and normalization using CO_2 injections

In order to compare amounts of liberated SO_2 during TG-MS between different measurements, the SO_2 peak areas, as measured with the MS, were normalized to the peak area resulting from CO_2 injections with a fixed amount of CO_2. The mean value of the peak areas of both CO_2 injections was calculated ($\frac{A_{CO_2-1}+A_{CO_2-2}}{2} = A_{CO_2-avg.}$) and the SO_2 peak area was divided by the sample specific $A_{CO_2-avg.}$. From the unitless quotient

($\frac{A_{SO2-sample}\ in\ V*s}{A_{CO_2-avg.-sample}\ in\ V*s}$) of each sample the quotient of the respective support ($\frac{A_{SO2-support}\ in\ V*s}{A_{CO2-avg.-support}\ in\ V*s}$) was subtracted. This final quotient for the untreated sample corresponds to 0 % of removed stabilizer. By subtracting the quotient of the other samples from the quotient of the untreated sample the relative amount of removed stabilizer is calculated.

1.4. Sample holder for the Au finder grids for electrochemical measurements

In order to perform electrochemical experiments, the Au finder grids where contacted as shown in SI Figure 1. The Au-finder grid is placed in the middle of the freshly polished glassy carbon electrode embedded in PTFE. Then a custom-made PTFE cap is placed on top of the GCE and pressed down to bring the carbon film of the Au-finder grid in strong contact with the GCE. In this way, the Au-finder grid is contacted over its whole area. The PTFE-embedded electrode may then be screwed to a standard electrode holder and is ready for electrochemical experiments-

SI Figure 1. Representation of the sample holder for the Au-finder grids with a costume made PTFE cap.

1.5. Additional Figures

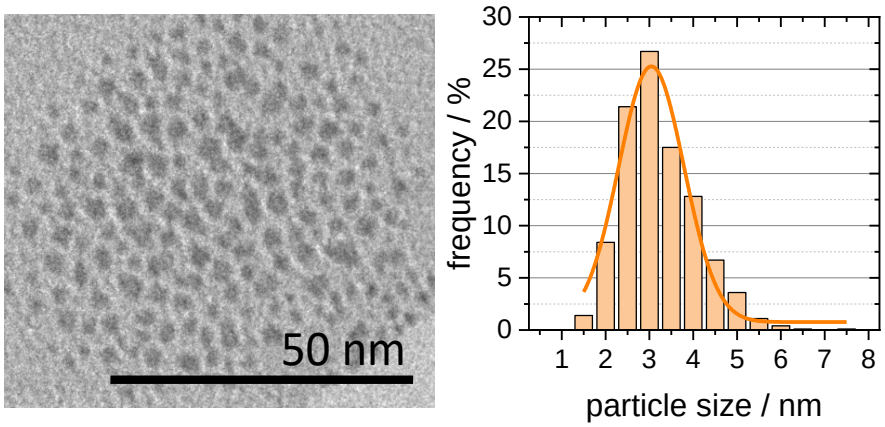

SI Figure 2. TEM image of the colloidal AuNPs and their size distribution (at least 1800 particles evaluated) with a Gaussian curve fitted.

SI Figure 2. shows a TEM image of the as prepared AuNPs (left) and the particle size distribution (right) of the AuNPs. Both represent the initial state of the AuNPs before any further steps (including deposition onto a support) were carried out.

SI Table 1. Size, size range, standard deviation and particles counted for TEM measurements of the treated powder samples, as well as the solid residue of the different carbon materials after the different treatments, for correction of the TG-MS measurements of the metal loading.

Sample	Treatment	Particle size (stdv.) / nm	Size range / nm	Particles measured	Au loading / wt.%	Solid residue of treated support / wt.%
Au-Vulcan	O_2	3.7 (± 1.2)	1.4–11.0	2375	18.1	1.7
	H_2	4.0 (± 1.9)	1.9-9.0	3062	17.1	1.4
	O_2+H_2	5.3 (± 1.9)	0.6-12.3	1464	25.0	0.8
	untreated	1.7 (± 0.4)	0.6-3.8	2381	16.8	0.5
Au-CNT	O_2	3.4 (± 1.7)	1.0-10.6	502	15.5	1.4
	H_2	4.8 (± 1.4)	1.7-9.4	489	15.0	1.9
	O_2+H_2	5.1 (± 2.3)	1.3-21.2	530	21.1	1.9
	untreated	2.0 (± 0.5)	0.6-3.9	514	14.6	0.8
Au-BP2000	O_2	2.9 (± 0.8)	1.1-6.3	516	16.7	1.2
	H_2	2.4 (± 0.7)	0.7-5.6	501	19.9	0.5
	O_2+H_2	3.6 (± 1.2)	1.2-8.5	611	24.9	0.5
	untreated	1.8 (± 0.5)	0.6-3.6	396	17.1	1.8

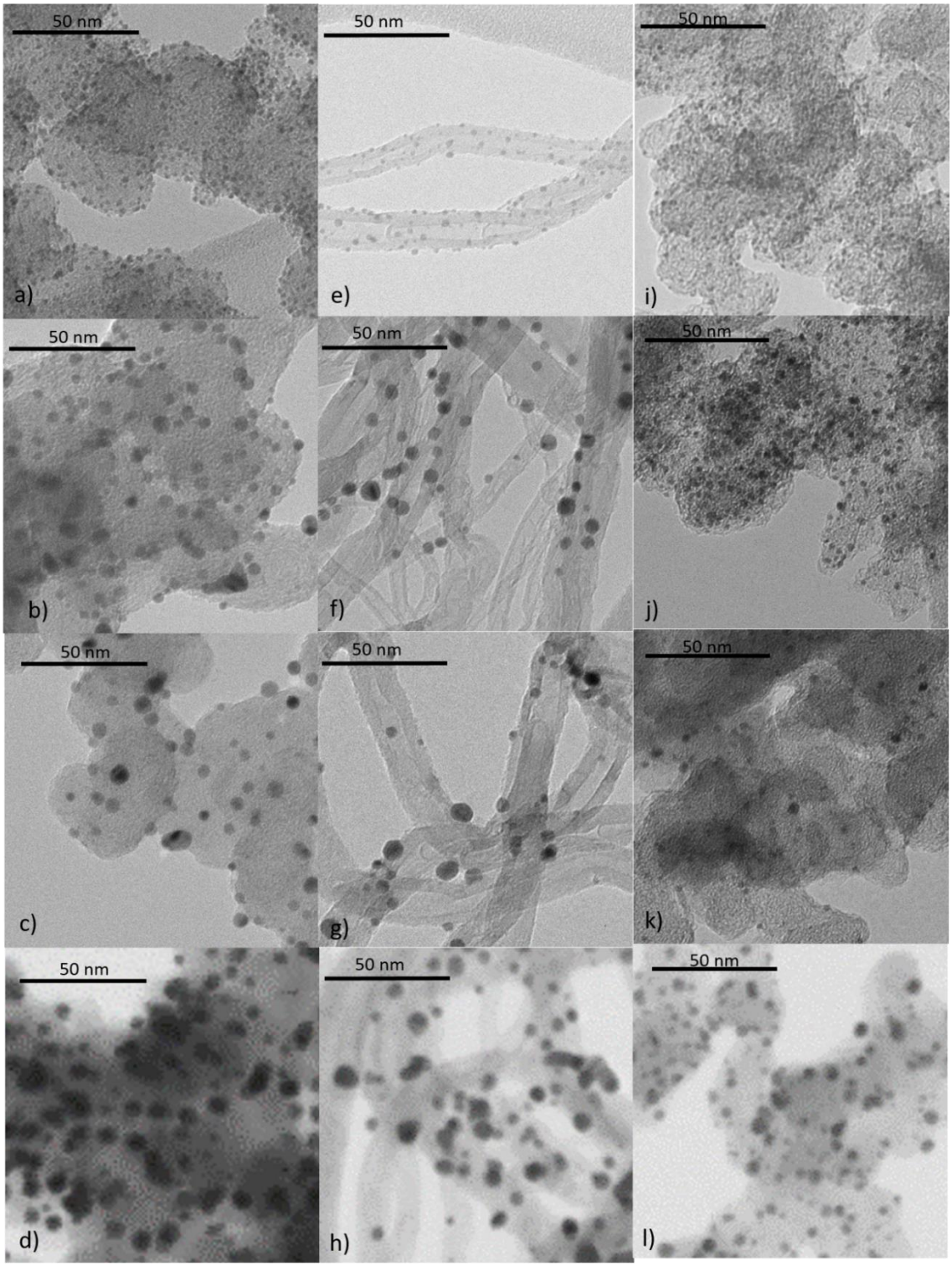

SI Figure 3. (S)TEM images of AuNP on Vulcan (a)-d)), on Baytubes (e)-h)) and on BP2000 (i)-l)). Top Row (a), e), i)) untreated; b), f), j) 300 °C 20% O_2/Ar treated, c), g), k) 400 °C 15% H_2/Ar; d), h), l) combined treatment).

SI Figure 3 presents (S)TEM images of the untreated and treated powder samples and the respective values are summarized in SI Table 1. The treatment-dependent particle growth, as described in the article is clearly visible.

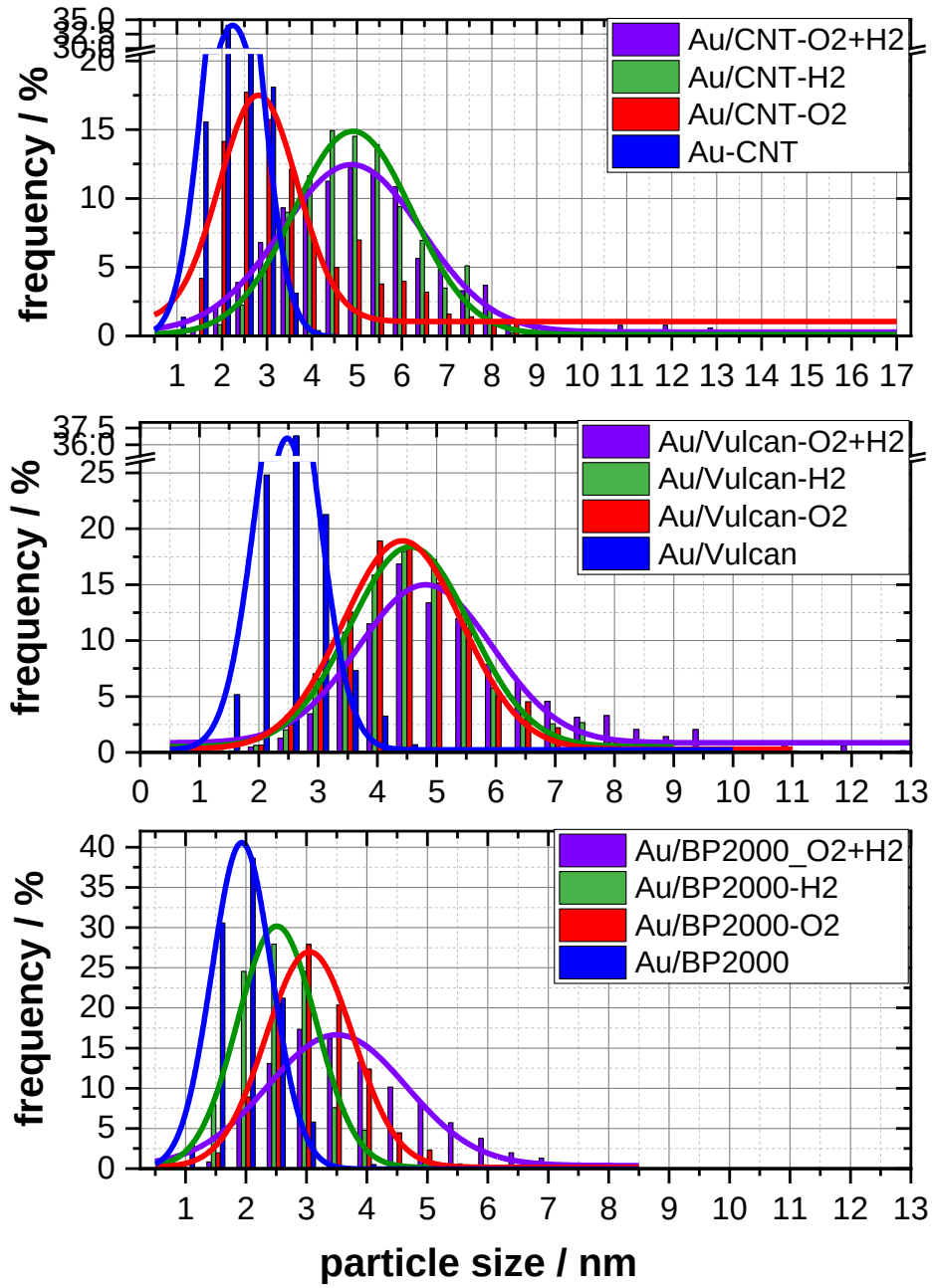

SI Figure 4. Particle size distribution according to different treatments and supporting materials a) Vulcan, b) CNT and c) BP2000 with the corresponding Gaussian curves fitted.

SI Figure 4 presents the particle sizes and size distributions of the different treated Au/C materials, corresponding to the data shown in Figure 3a) in the main article and showing that the AuNP exhibit a Gaussian-type particle size distribution around the average particle size.

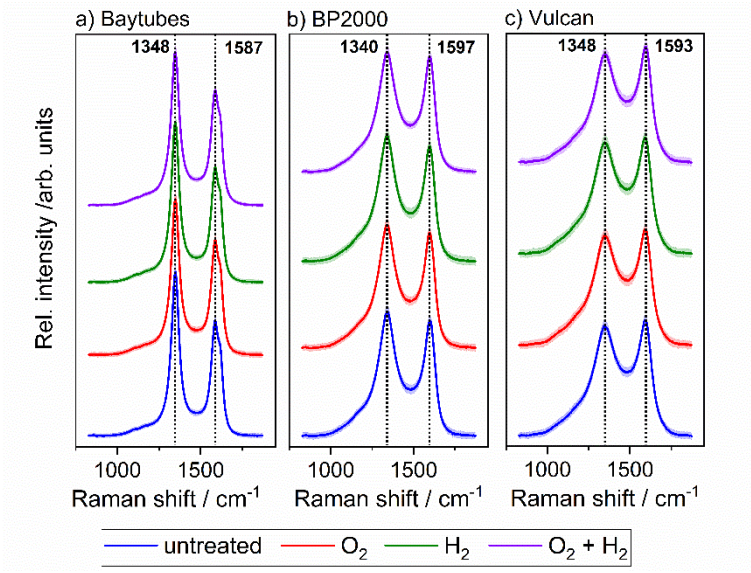

SI Figure 5. Averaged spectra of the Raman mapping measurements of the different treated samples, dotted lines D-Band (~1345 cm^{-1}) and G-Band (~1585 cm^{-1}).

Si Figure 5 presents the results of Raman mapping measurements. These measurements underline the differences in the Raman spectra of the investigated samples, which result from their different structural features, as well as the impact of the treatments onto the carbon materials. The G-Band (~1585 cm^{-1}) represents the share of graphitic carbon and the D-Band (~1345 cm^{-1}) indicates the shares of disordered carbon.[1,2]

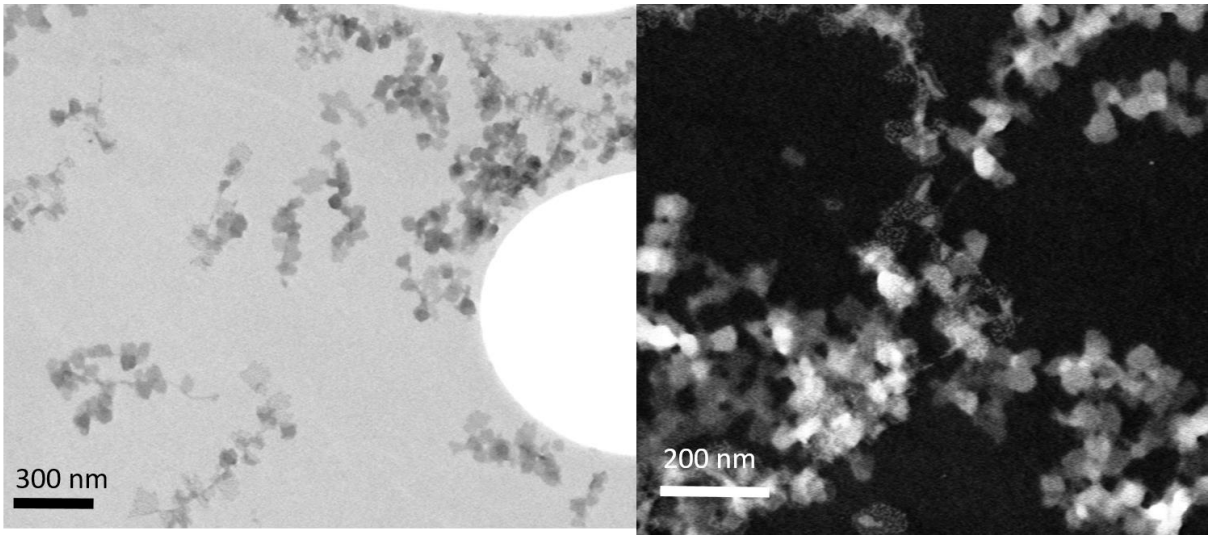

SI Figure 6. STEM images of pure 1-dodecanthiol. Left: full STEM detector, right: dark field contrast with only the outer rings of the STEM detector to visualize a higher contrast.

SI Figure 6 presents STEM images of the stabilizing agent 1-dodecanthiol to check if excess stabilizing agent is present in the samples. The dark field contrast image presents a higher contrast for regions of higher electron density. The quite homogeneous contrast shows that there are no materials with high electron density (e.g. metals) involved in the presented samples.

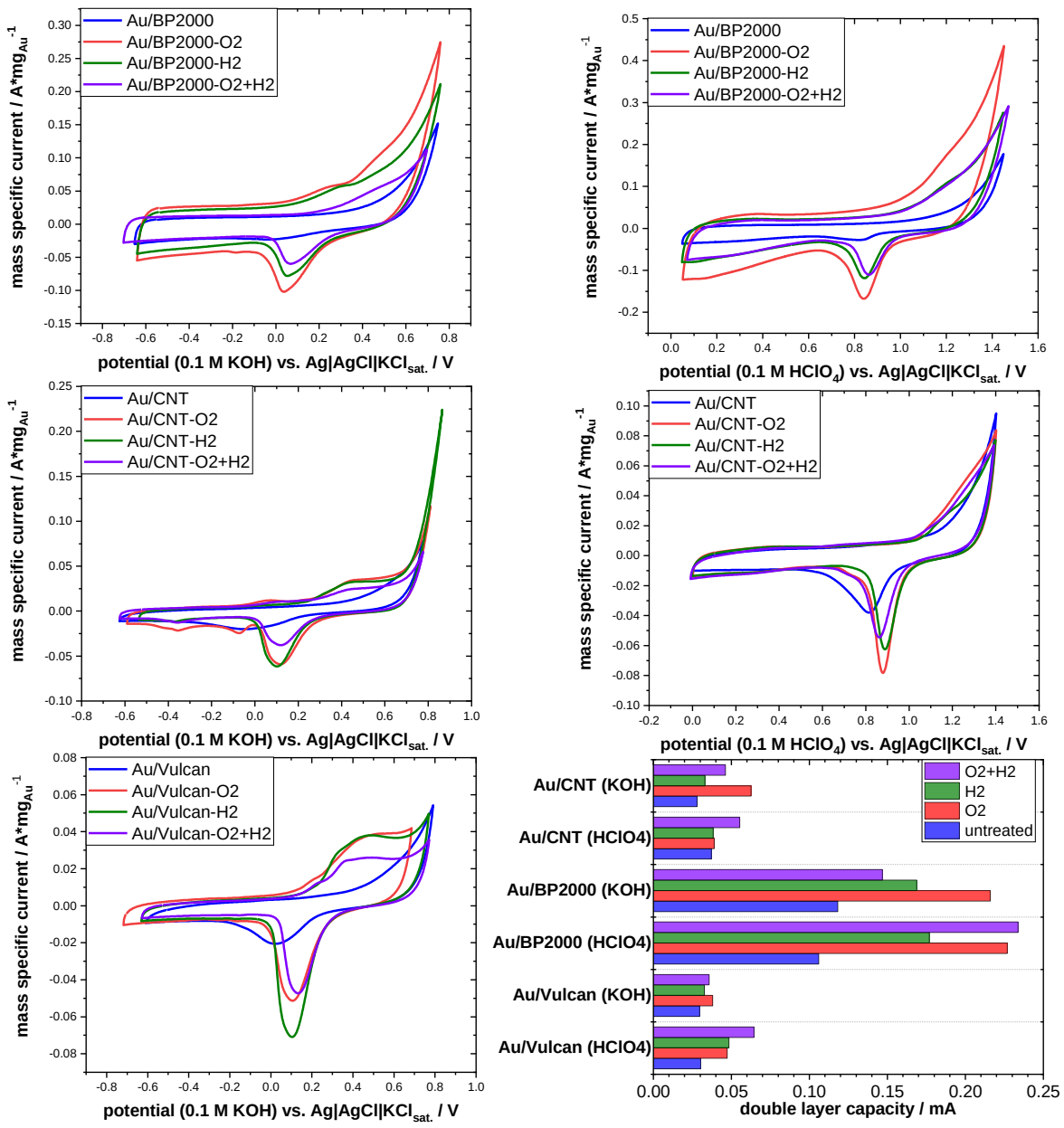

SI Figure 7. 3rd CV of the different samples in 0.1 M $HClO_4$ and 0.1 M KOH, respectively, as well as the double layer capacity of all samples in the different electrolytes obtained from the 3rd CV.

SI Figure 7 presents CVs of all samples, treated and untreated, in 0.1 M KOH and of the BP2000 and the CNT sample in 0.1 M $HClO_4$ and the double layer capacity of all samples in 0.1 M KOH and 0.1 M $HClO_4$. The figure clearly demonstrates the different behavior caused by the different support materials and the rather similar behavior of each individual material after the different treatments.

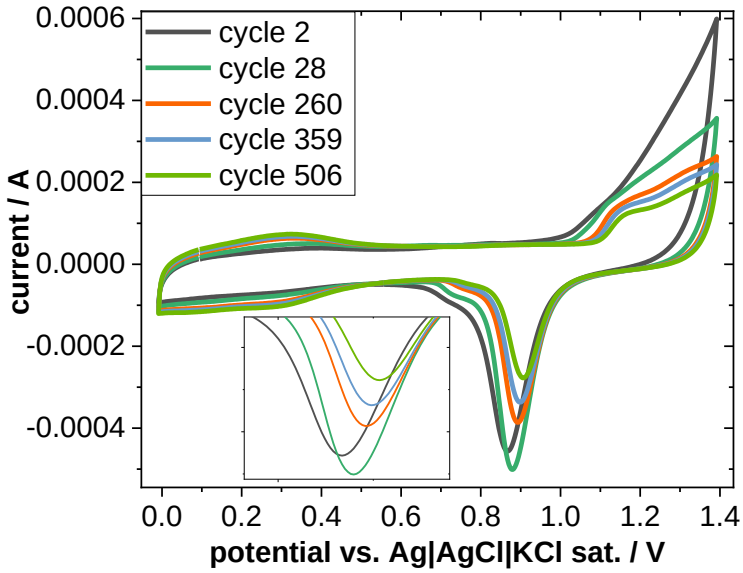

SI Figure 8. Representative CVs showing a degradation experiment of Au/CNT-O_2+H_2 in 0.1 M $HClO_4$ with an enlarged view of the Au-reduction peak in the inset.

SI Figure 8 presents selected cycles of a CV measurement of Au/CNTs which were treated with the combined treatment. Initially a current increase can be observed for the Au reduction peal (cycle 2 to 28) followed by a current decrease. Prolonged cycling for 1000 cycles led to the disappearance of the gold redox features (not shown).

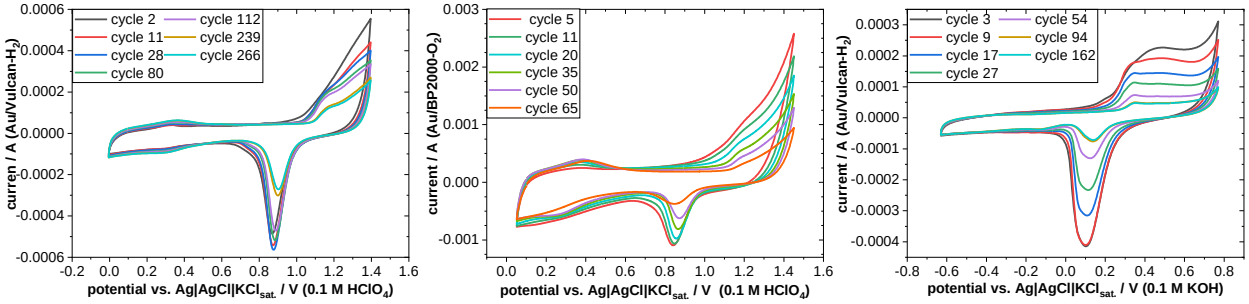

SI Figure 9. Representative CVs of degradation experiments for Au/Vulcan-H_2 in 0.1 M $HClO_4$ (left), Au/BP2000-O_2 in 0.1 M $HClO_4$ (middle) and Au/Vucan-H_2 in 0.1 M KOH (right)

SI Figure 9 presents further representative degradation CVs. The comparison between the measurements of Au/Vulcan-H_2 in 0.1 M $HClO_4$ and 0.1 M KOH (left and right graph in SI Figure 8) underlines that in KOH no additional peaks appear, whereas in 0.1 M $HClO_4$ a redox peak pair develops between 0.2 and 0.4 V, which is typically attributed to quinone-type redox features of the carbon support. Similar peaks are visible in other measurements in 0.1 M $HClO_4$ (cf. SI Figure 7 and SI Figure 8, middle). Such quinone-type surface groups at the support (pseudo-capacitive in nature) can be found after chemical oxidation of a bare CNT support as well[3].

However, since there is no increase in the double layer capacity, one may assume that existing edges and corners are oxidized during the CVs. Considering the lower thermal stability of the carbon support in the presence of AuNPs (see TG-MS results in the main article) an electrocatalytic activity of AuNPs for the carbon oxidation may be proposed.

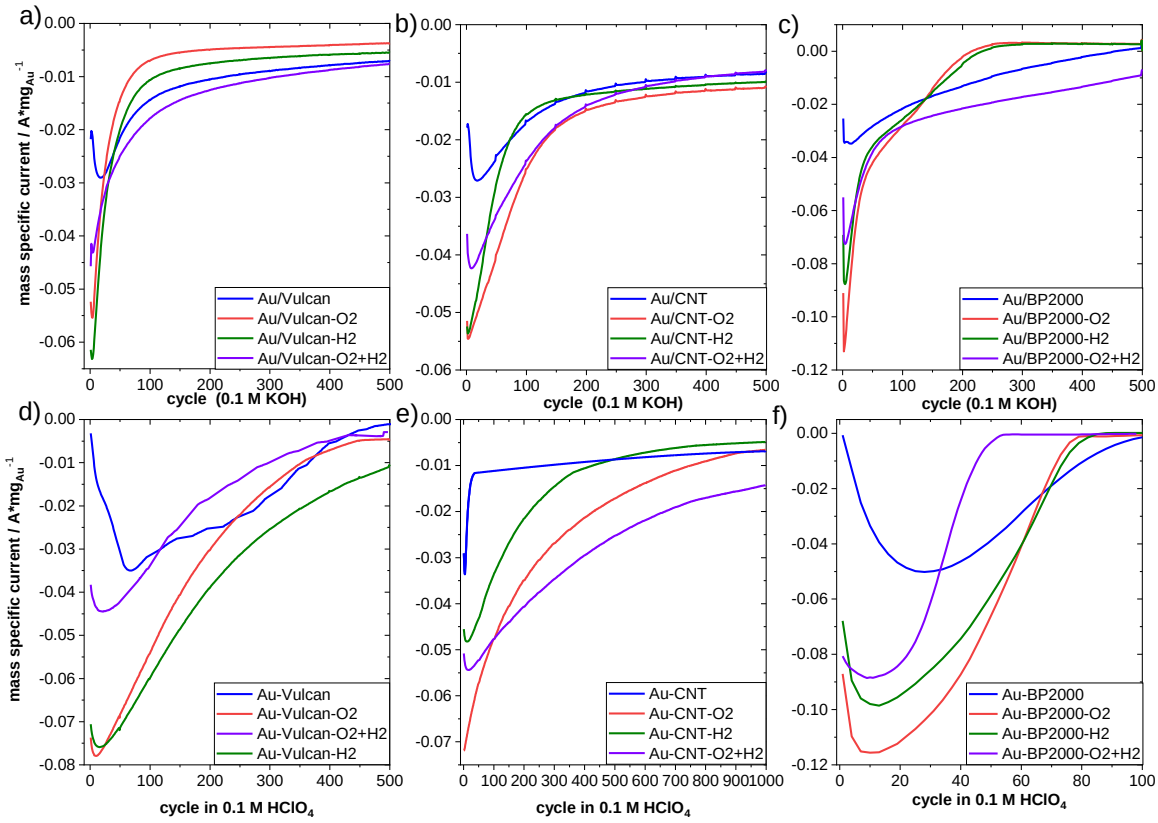

SI Figure 10. Average (three repeated measurements) Au-mass specific current of the Au-reduction peak over the number of degradation CV cycles.

Si Figure 10 shows the development of the Au-reduction peak minimum with ongoing degradation CVs. A different degradation behavior can be observed for the various samples.

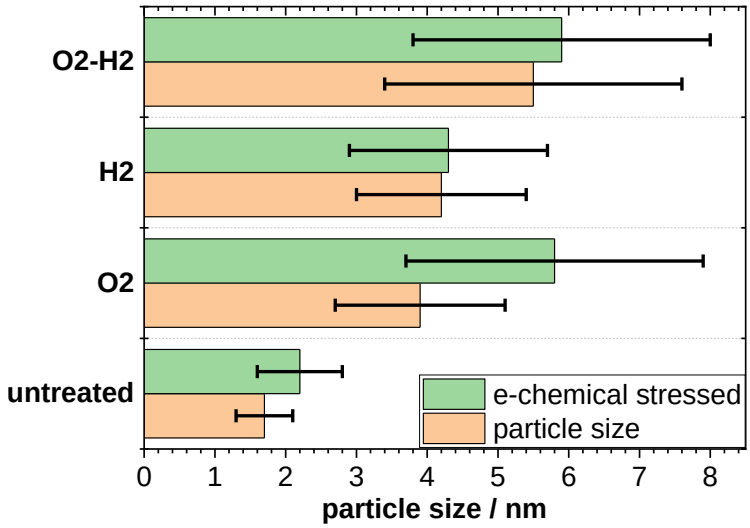

SI Figure 11. Development of particle sizes and size distributions of the electrochemically stressed samples as obtained from il-(S)TEM investigations

SI Figure 11 displays the particle growth during the electrochemical stress procedure of Auf/C catalysts on the Au-finder grids as well as the standard deviation of the particle sizes, which is increased after electrochemical stress.

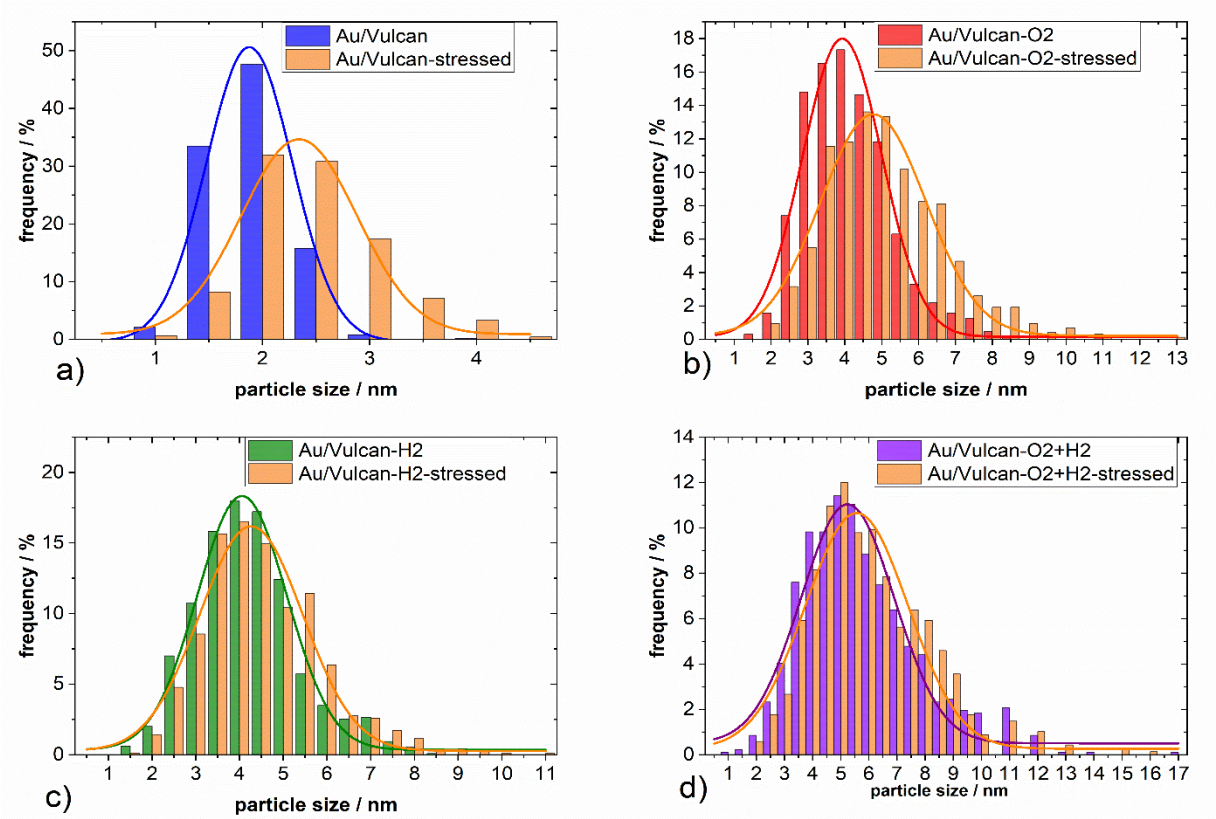

SI Figure 12. Particle size distribution of untreated a), O_2- b), H_2- c) and O_2+H_2-treated Au/Vulcan before and after electrochemical stress in 0.1 M KOH.

Si Figure 12 shows the particle size distribution of the untreated and treated Au/Vulcan samples before and after electrochemical stress on the Au-finder grids in 0.1 M KOH. While SI Figure 10 intends to provide an easier comparison between the samples, SI Figure 11 gives a more detailed view on the changes of particle sizes and underlines the loss of smaller particles and the wider particle size distribution.

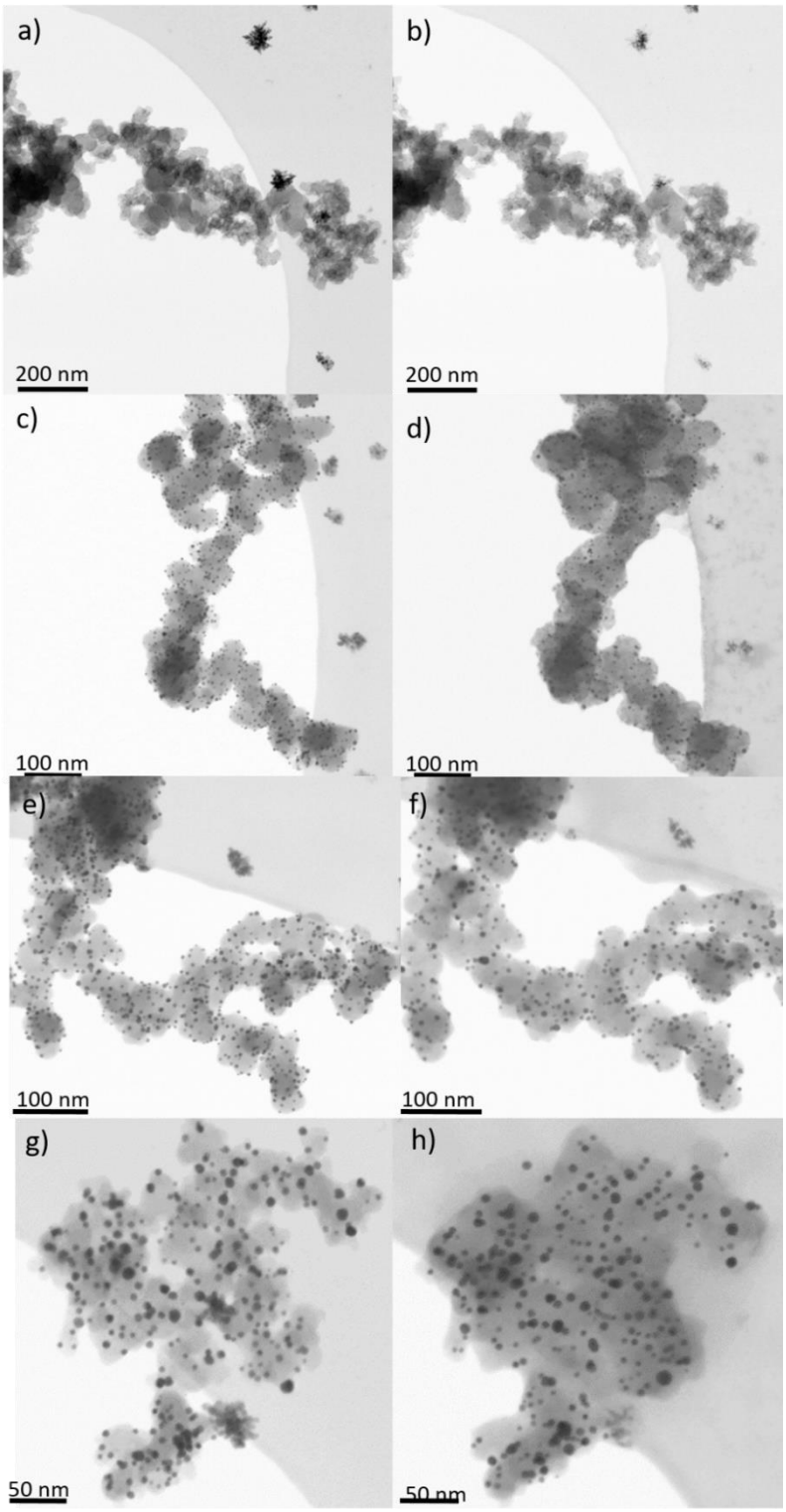

SI Figure 13. il- (S)TEM images of Au/Vulcan before being subjected to electrochemical stress, un- a), O_2- c), H_2- e) and O_2+H_2-treated g) and after subjection to electrochemical stress un- b), O_2- d), H_2- f) and O_2+H_2-treated h).

SI Figure 13 presents il-(S)TEM images of lower magnification to assess possible changes in the carbon support structure. However very obviously only very minor changes occur to the support during electrochemical stress.

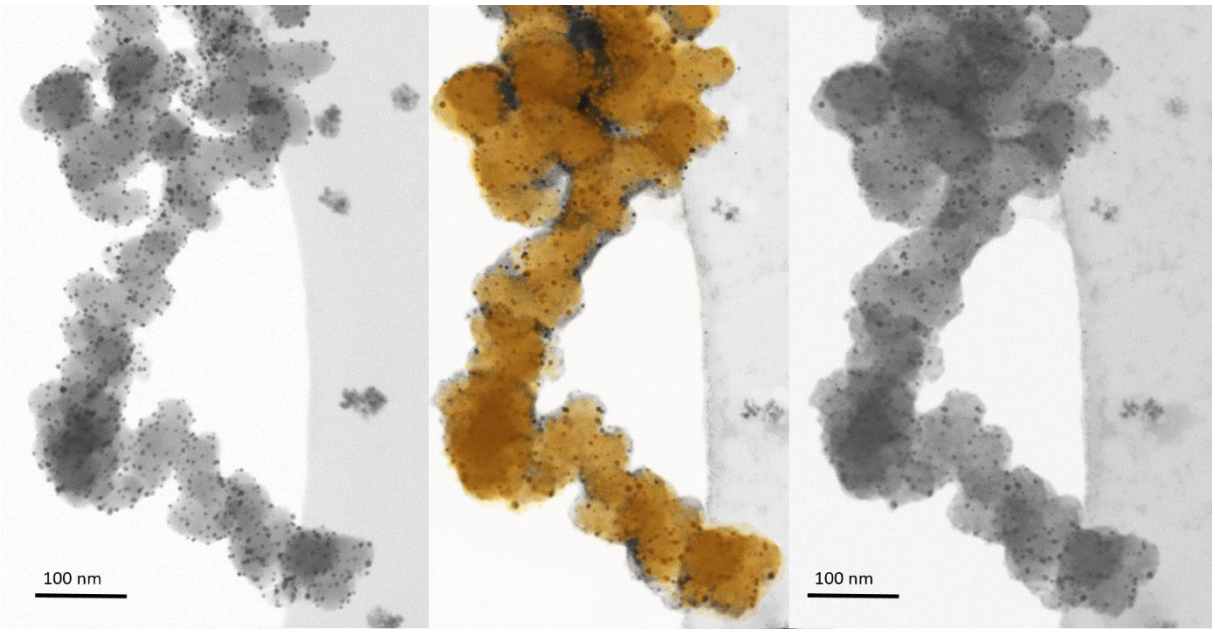

SI Figure 14. STEM images of Au/Vulcan before (left) and after (right) electrochemical stress. The figure in the middle provides an overlay of both images where the sample after electrochemical stress treatment is displayed in orange.

However, interestingly there is kind of a swelling of the carbon support observable (SI Figure 13 and 14). This could be due to KOH from the electrolyte which is remaining after the electrochemical treatment, but also could be a bloat of the carbon structure due to intercalation or defects resulting from the electrochemical carbon oxidation. However, since there is no obvious loss or drastically change nor change of the double layer capacity this should rule out strong support changes or material loss as degradation mechanism.

References

1 M. M. Lucchese, F. Stavale, E. M. Ferreira, C. Vilani, M.V.O. Moutinho, R. B. Capaz, C. A. Achete and A. Jorio, *Carbon*, 2010, **48**, 1592–1597.

2 A. Sadezky, H. Muckenhuber, H. Grothe, R. Niessner and U. Pöschl, *Carbon*, 2005, **43**, 1731–1742.

3 M. Steimecke, S. Rümmler and M. Bron, *Electrochim. Acta*, 2015, **163**, 1–8.